

## Bloom-Gilman duality of inelastic structure functions in nucleon and nuclei

G. Ricco,<sup>1,2</sup> M. Anghinolfi,<sup>2</sup> M. Ripani,<sup>2</sup> S. Simula,<sup>3</sup> and M. Taiuti<sup>2</sup>

<sup>1</sup>*Dipartimento di Fisica, Università di Genova, Via Dodecanneso 33, I-16146, Genova, Italy*

<sup>2</sup>*Istituto Nazionale di Fisica Nucleare, Sezione di Genova, Via Dodecanneso 33, I-16146, Genova, Italy*

<sup>3</sup>*Istituto Nazionale di Fisica Nucleare, Sezione Sanità, Viale Regina Elena 299, I-00161 Roma, Italy*

(Received 5 March 1997)

The Bloom-Gilman local duality of the inelastic structure function of the proton, the deuteron, and light complex nuclei is investigated using available experimental data in the squared four-momentum transfer range from 0.3 to 5 (GeV/c)<sup>2</sup>. The results of our analysis suggest that the onset of the Bloom-Gilman local duality is anticipated in complex nuclei with respect to the case of the proton and the deuteron. A possible interpretation of this result in terms of a rescaling effect is discussed with particular emphasis on the possibility of reproducing the damping of the nucleon-resonance transitions observed in recent electroproduction data off nuclei. [S0556-2813(98)00901-7]

PACS number(s): 13.60.Hb, 13.60.Rj, 12.40.Nn, 14.20.Dh

### I. INTRODUCTION

The investigation of inelastic lepton scattering off nucleon and nuclei can provide relevant information on the concept of parton-hadron duality, which deals with the relation among the physics in the nucleon-resonance and deep inelastic scattering (DIS) regions. As is known, well before the advent of QCD, parton-hadron local duality was observed empirically by Bloom and Gilman [1] in the structure function  $\nu W_2^p(x, Q^2)$  of the proton measured at SLAC (where  $x \equiv Q^2/2m\nu$  is the Bjorken scaling variable,  $m$  the nucleon mass, and  $Q^2$  the squared four-momentum transfer). Moreover, it is well established that both the electroexcitation of the most prominent nucleon resonances and the nuclear structure function in the DIS region are affected by nuclear medium (cf., e.g., Refs. [2,3]). In particular, existing data on the electroproduction of nucleon resonances show that the disappearing of the resonance bumps with increasing  $Q^2$  is faster in nuclei than in the nucleon (cf., e.g., Refs. [4,5] and references therein). Therefore, in this paper we want to address the specific question of whether and to what extent the Bloom-Gilman duality already observed in the proton occurs also in the structure function of a nucleus. To this end, all the available experimental data for the structure functions of the proton, the deuteron, and light complex nuclei in the  $Q^2$  range from 0.3 to 5 (GeV/c)<sup>2</sup> have been analyzed and the  $Q^2$  behaviors of the structure function and its moments are presented for all the targets considered. In the case of the proton we observe that the Bloom-Gilman local duality is fulfilled only by the inelastic part of the structure function, while the inclusion of the contribution of the elastic peak leads to remarkable violations of the local duality. In the case of complex nuclei, despite the poor statistics of the available data, it is found that the onset of the parton-hadron local duality for the inelastic part of the structure function is anticipated with respect to the case of the proton and the deuteron. Nevertheless, new high-precision nuclear data are needed and, in this respect, it should be mentioned that the Thomas Jefferson National Accelerator Facility (TJNAF) is expected to provide in the near future systematic measurements with unprecedented accuracy of the nucleon and

nuclear inelastic response to electron probes in the region of nucleon-resonance production for values of  $Q^2$  up to several (GeV/c)<sup>2</sup>. Finally, a possible interpretation of the observed nuclear modification of the onset of the Bloom-Gilman local duality in terms of a  $Q^2$ -rescaling effect is discussed with particular emphasis on the possibility of reproducing the damping of the nucleon-resonance transitions observed in recent electroproduction data off nuclei [5].

### II. DUAL STRUCTURE FUNCTION

The Bloom-Gilman local duality [1] states that the smooth scaling curve measured in the DIS region at high  $Q^2$  represents an average over the resonance bumps seen in the same  $x$  region at low  $Q^2$ . More precisely, Bloom and Gilman pointed out the occurrence of a precocious scaling of the average of the inclusive  $\nu W_2^p(x', Q^2)$  data in the resonance region to the DIS structure function  $F_2^p(x')$ , at corresponding values of an improved empirical variable  $x' = x/(1 + m^2x/Q^2)$ . Later on, within QCD, a justification of the Bloom-Gilman duality was offered by De Rujula, Georgi, and Politzer [6] in terms of the moments  $M_n(Q^2)$  of the nucleon structure function  $F_2(\xi, Q^2)$ :

$$M_n(Q^2) \equiv \int_0^1 d\xi \xi^{n-2} F_2(\xi, Q^2), \quad (1)$$

where  $\xi$  is the Nachtmann variable (cf. [7]),

$$\xi = \frac{2x}{1 + \sqrt{1 + 4m^2x^2/Q^2}}. \quad (2)$$

Using the operator product expansion (OPE) the authors of Ref. [6] argued that

$$M_n(Q^2) = A_n(Q^2) + \sum_{k=1}^{\infty} \left( n \frac{\gamma^2}{Q^2} \right)^k B_{nk}(Q^2), \quad (3)$$

where  $\gamma^2$  is a scale constant. The first term  $A_n(Q^2)$  in Eq. (3) is the result of perturbative QCD, while the remaining terms  $B_{nk}(Q^2)$  are higher twists related to parton-parton correla-

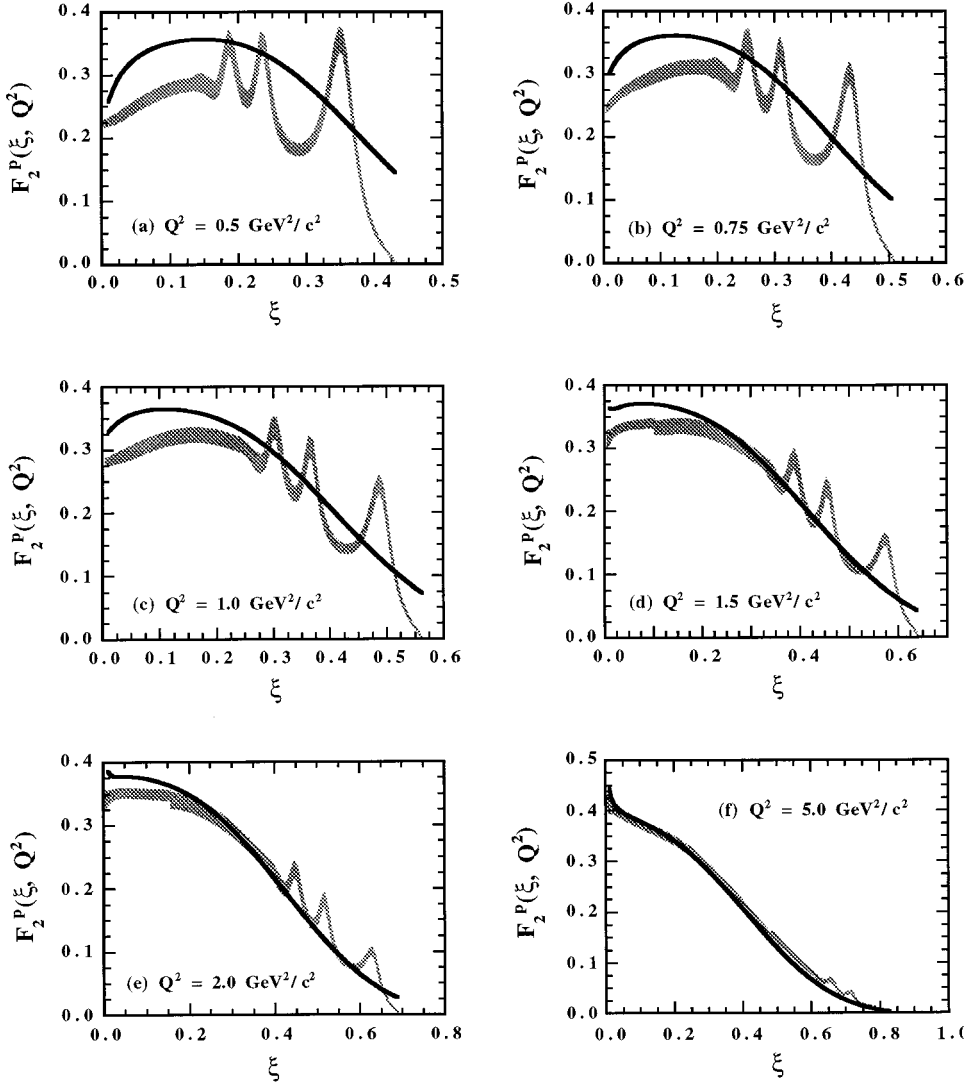


FIG. 1. Proton structure function  $F_2^P(\xi, Q^2) = \nu W_2^P(\xi, Q^2)$  versus the Nachtmann variable  $\xi$  [Eq. (2)] at various values of  $Q^2$ . The shaded areas represent the pseudo-data, obtained from a fit of SLAC data at medium and large  $x$  [15] and from a fit of NMC data [9] in the DIS region, including the total uncertainty of the fits. The solid lines are the *dual* structure function of the nucleon [Eq. (4)], obtained starting from the GRV [11] parton densities evolved NLO at low  $Q^2$  and target mass corrected according to Ref. [7].

tions. The value of  $\gamma^2$  is relatively small (a recent estimate, made in Ref. [8], yields  $\gamma^2 \sim 0.1 - 0.3 \text{ GeV}^2$ ). Therefore, at  $Q^2 \geq m^2$  the asymptotic moments  $A_n(Q^2)$  are still leading, while resonances contribute to the higher twists  $B_{nk}(Q^2)$ . The quantities  $A_n(Q^2)$  can be considered as the moments of a smooth structure function, which can be identified with the average function  $\langle \nu W_2(x, Q^2) \rangle$  occurring in the Bloom-Gilman local duality, namely [7],

$$\begin{aligned}
 \langle \nu W_2(x, Q^2) \rangle &= \frac{x^2}{(1 + 4m^2 x^2 / Q^2)^{3/2}} \frac{F_2^S(\xi, Q^2)}{\xi^2} \\
 &+ 6 \frac{m^2}{Q^2} \frac{x^3}{(1 + 4m^2 x^2 / Q^2)^2} \int_{\xi}^1 d\xi' \frac{F_2^S(\xi', Q^2)}{\xi'^2} \\
 &+ 12 \frac{m^4}{Q^4} \frac{x^4}{(1 + 4m^2 x^2 / Q^2)^{5/2}} \\
 &\times \int_{\xi}^1 d\xi'' \int_{\xi'}^1 d\xi''' \frac{F_2^S(\xi''', Q^2)}{\xi'''^2}, \quad (4)
 \end{aligned}$$

where the  $\xi$  dependence as well as the various integrals appearing in the right-hand side (RHS) account for target mass

effects in the OPE of the hadronic tensor. According to Ref. [7] these effects have to be included in order to cover the low- $Q^2$  region. In Eq. (4),  $F_2^S(x, Q^2)$  represents the asymptotic nucleon structure function, fitted to high- $Q^2$  proton and deuteron data [9] and extrapolated down to low values of  $Q^2$  by the Altarelli-Parisi evolution equations [10]. In this paper the Gluck-Reya-Vogt (GRV) fit [11], which assumes a renormalization scale as low as  $0.4 \text{ (GeV}/c)^2$ , will be used to obtain the parton densities  $\rho_f(x, Q^2)$  evolved at next to leading order (NLO) from sufficiently low  $Q^2$  to cover the range of interest in the present analysis. In the DIS region [12] one gets  $F_2^S(x, Q^2) = \sum_f e_f^2 x [\rho_f(x, Q^2) + \bar{\rho}_f(x, Q^2)]$ .

In what follows, we will refer to the mass-corrected, NLO-evolved function (4) as the *dual* structure function of the nucleon. We stress that by definition the *dual* function does not contain any higher twists generated by parton-parton correlations, i.e., the twists related to the moments  $B_{nk}(Q^2)$  in Eq. (3). It should be mentioned that Eq. (4) suffers from a well-known [13,14] mismatch; indeed, since  $\xi(x=1) = 2/(1 + \sqrt{1 + 4m^2/Q^2}) < 1$ , the RHS of Eq. (4) remains positive, while its LHS vanishes, as  $x$  approaches the elastic end point  $x=1$ . An alternative approach [13], limited

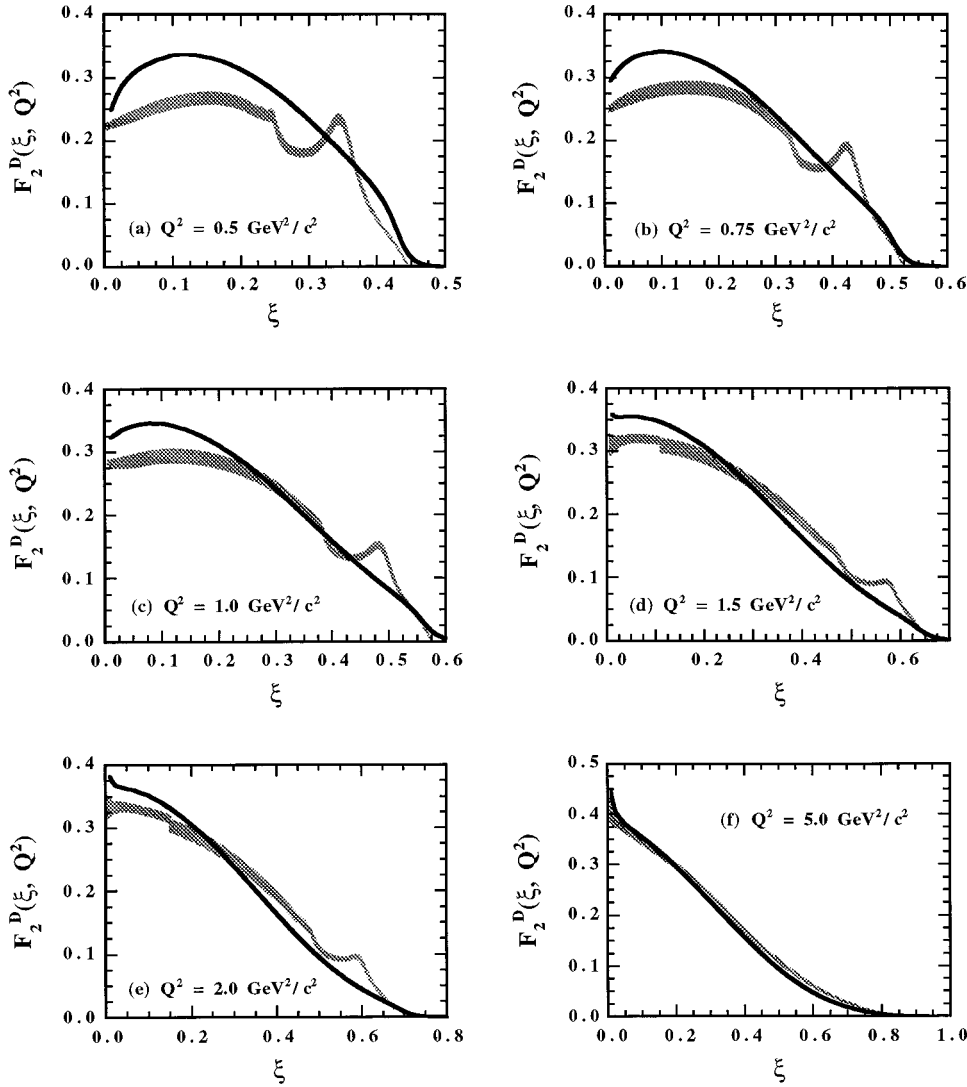


FIG. 2. The same as in Fig. 1, but for the deuteron structure function per nucleon  $F_2^D(\xi, Q^2) \equiv \nu W_2^D(\xi, Q^2)/2$ . The NMC data of Ref. [19] at low  $\xi$  and the fits of inclusive data given in Refs. [9] and [15] have been considered. The solid curve is the *dual* structure function of the nucleon [Eq. (4)], folded according to the procedure of Ref. [16], with the nucleon momentum distribution in the deuteron corresponding to the Paris nucleon-nucleon potential [18].

at the twist-4 order, is well behaved at the kinematical  $x = 1$  threshold, but it cannot be extrapolated to low values of  $Q^2$ , because an expansion over the quantity  $m^2 x^2/Q^2$  is involved. Moreover, inelastic threshold effects, due to finite pion mass, are accounted for neither in the  $Q^2$  evolution nor in the target mass corrections, because they are basically higher-twist effects; then, in order to make a detailed comparison with experimental data in the low- $Q^2$  region, we set the *dual* structure function (4) to zero at  $x \geq x_{\text{th}}$ , where

$$x_{\text{th}} = \frac{1}{1 + (m_\pi^2 + 2m_\pi m)/Q^2}, \quad (5)$$

with  $m_\pi$  being the pion mass. Therefore, the investigation of parton-hadron local duality will be limited to values of  $x$  not larger than  $x_{\text{th}}$ , Eq. (5), and to a  $Q^2$  range between a minimum value  $Q_{\text{min}}^2$ , which is of the order of the mass scale  $\mu^2$  where the moments of the structure functions  $M_n(Q^2)$  start to evolve according to twist-2 operators, and a maximum value  $Q_{\text{max}}^2 [\geq 5 \text{ (GeV/c)}^2]$  [8]], where the resonance contribution to the lowest moments of Eq. (3) is of the same order of magnitude of the experimental errors.

### III. INCLUSIVE DATA ANALYSIS

The pseudodata for the proton structure function  $\nu W_2^p$ , obtained from a fit of SLAC data at medium and large  $x$  [15] and from a fit of the NMC data [9] in the DIS region, are reported in Fig. 1 versus the Nachtmann variable  $\xi$ , Eq. (2), and compared with the *dual* structure function (4) at fixed values of  $Q^2$  in the range 0.5–2 (GeV/c)<sup>2</sup>. As already pointed out in [6], the onset of local duality occurs at  $Q^2 \approx Q_0^2 \sim 1-2 \text{ (GeV/c)}^2$ .

In case of the deuteron the average nucleon structure function  $\nu \bar{W}_2^N \equiv (\nu W_2^p + \nu W_2^n)/2$ , obtained from Eq. (4), should be folded with the momentum distribution which accounts for the internal motion of the nucleon in the deuteron. The most evident effect of this folding is a broadening of the nucleon elastic peak occurring at  $x = 1$  into a wider quasi-elastic peak, partially overlapping the inelastic cross section at large  $x$ . In the deuteron the nucleon momentum distribution is relatively narrow and this fact limits the overlap to the kinematical regions corresponding to  $x \geq 0.8$ . Therefore, it is still possible to subtract the quasielastic contribution directly from the total cross section [15]. The folding of the *dual* structure function of the nucleon [Eq. (4)] with the nucleon

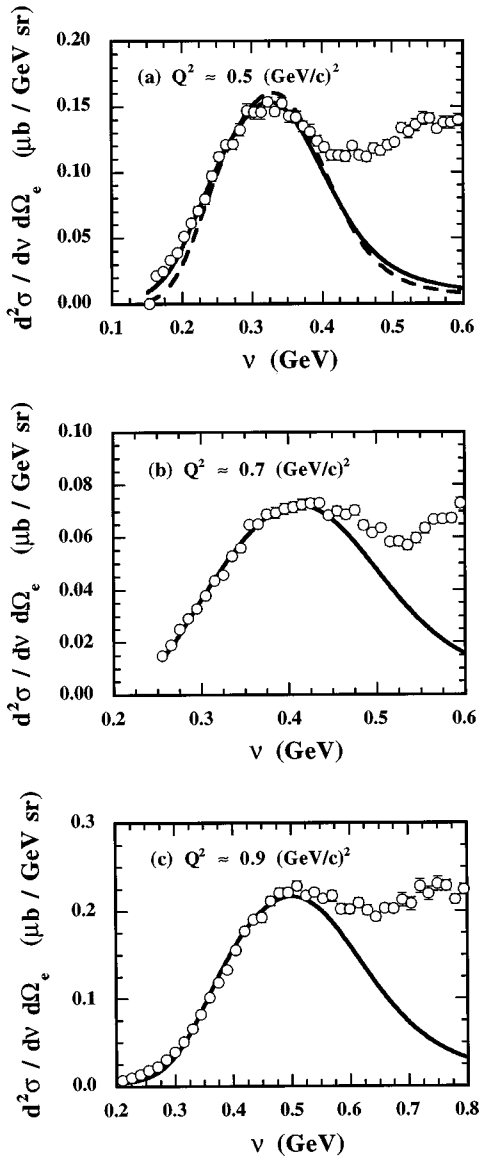


FIG. 3. Differential cross section (per nucleon) for the inclusive process  $^{12}\text{C}(e, e')X$  versus the energy transfer  $\nu$  in the  $Q^2$  range 0.5 – 0.9  $(\text{GeV}/c)^2$  (at the quasielastic peak). The solid lines represent the quasielastic contribution calculated using the approach of Ref. [25], which includes final state interaction effects. In (a) the dashed line is the same as the solid line, but obtained within the impulse approximation only, i.e., without including final state interaction effects. In (a), (b), and (c) the electron beam energy and scattering angle  $(E_e, \theta_e)$  are (1.3 GeV,  $37.5^\circ$ ), (1.5 GeV,  $37.5^\circ$ ), and (3.595 GeV,  $16^\circ$ ), respectively. In (a) and (b) the experimental data are from Ref. [24] (c), while in (c) they are from Ref. [24] (a).

momentum distribution in the deuteron is performed following the procedure of Ref. [16], which can be applied both at low and high values of  $Q^2$ , at variance with the standard high- $Q^2$  folding of Ref. [17]. Adopting the deuteron wave function corresponding to the Paris nucleon-nucleon potential [18], our results for the *dual* structure function folded in the deuteron are reported in Fig. 2 at fixed values of  $Q^2$  in the range 0.5–2  $(\text{GeV}/c)^2$ , and compared with the deuteron structure function per nucleon,  $F_2^D(\xi, Q^2) \equiv \nu W_2^D(\xi, Q^2)/2$ , obtained from the NMC data [19] at low  $\xi$  and the fits of inclusive data given in Refs. [9] and [15].

Despite the smoothening of nucleon resonances caused by the Fermi motion, parton-hadron local duality appears to start again at  $Q^2 \approx Q_0^2 \sim 1-2$   $(\text{GeV}/c)^2$ .

In the case of complex nuclei the analysis of existing inclusive data is complicated by different reasons.

(i) Inclusive data, coming mainly from old experiments generally with poor statistics, is still very fragmented.

(ii) The longitudinal to transverse separation has been done only in case of few measurements carried out in the nucleon-resonance region. An experiment performed at  $Q^2 = 0.1$   $(\text{GeV}/c)^2$  [20] in  $^{12}\text{C}$  and  $^{56}\text{Fe}$  claims a longitudinal to transverse ratio compatible with zero inside experimental errors ( $\sim 10\%$ ), while at  $Q^2 \gtrsim 1$   $(\text{GeV}/c)^2$  deep inelastic scattering data are consistent with larger, fairly  $x$  independent  $\sigma_L/\sigma_T$  ratios [21]. However, the sensitivity of the extraction of the nuclear structure function  $\nu W_2^A$  from the total cross section to the longitudinal to transverse ratio turns out to be rather small (not larger than a few percent when  $\sigma_L/\sigma_T$  is moved from zero to 20% in the worst kinematical conditions). Therefore, we have simply interpolated all the existing data for  $\sigma_L/\sigma_T$  in proton and nuclei, averaged on  $x$ , as a function of  $Q^2$  only, obtaining the following empirical ratio:

$$\sigma_L/\sigma_T = aQ^2[e^{-bQ^2} + ce^{-dQ^2}],$$

with  $a = 0.014$ ,  $b = 0.07$ ,  $c = 40.8$ , and  $d = 0.78$ . Since the observed dependence of the inclusive nuclear data on the mass number  $A$  is weak [22], the nuclear structure function  $\nu W_2^A$  has been determined as a function of  $\xi$  for fixed  $Q^2$  bins using data for  $^9\text{Be}$  [22,23],  $^{12}\text{C}$  [15,19,24], and  $^{16}\text{O}$  [5]. Therefore, our result could be considered representative of a complex nucleus with  $A \approx 12$ .

(iii) Since the nucleon momentum distribution is wider in complex nuclei than in the deuteron (cf. [25] and references therein), the quasielastic contribution strongly overlaps the inelastic cross section at low values of  $Q^2$ ; moreover, the quasielastic peak is known to be affected by final state interaction effects at  $Q^2 \lesssim 0.5$   $(\text{GeV}/c)^2$  (cf. [5]). Then, the subtraction of the quasielastic contribution is more critical in nuclei.

(iv) Nucleon binding can affect nuclear structure function and should be properly taken into account [3];

The calculation of the quasielastic contribution has been performed following the approach of Ref. [25], which has been positively checked against SLAC data at values of  $Q^2$  of a few  $(\text{GeV}/c)^2$  [25] as well as against jet-target data at lower  $Q^2$  [down to 0.1  $(\text{GeV}/c)^2$  [5]]. An example of the quality of the agreement among the parameter-free predictions of the quasielastic contribution to the inclusive  $^{12}\text{C}(e, e')X$  cross section and available data at the quasielastic peak and in its low-energy side for a  $Q^2$  range 0.5–1  $(\text{GeV}/c)^2$  is shown in Fig. 3. Furthermore, the *dual* structure function of the nucleon, Eq. (4), has been folded using again the procedure of Ref. [16], which, in the case of complex nuclei, involves the nucleon spectral function of Ref. [25]; in this way binding effects are taken into account for states both below and above the Fermi level.

After quasielastic subtraction, the results obtained for the inelastic nuclear structure function per nucleon,  $F_2^A(\xi, Q^2) \equiv \nu W_2^A(\xi, Q^2)/A$ , are shown in Fig. 4 for various  $Q^2$  bins, namely,  $Q^2 = 0.375 \pm 0.03$ ,  $0.50 \pm 0.05$ ,  $0.75 \pm 0.05$ ,  $1.1 \pm 0.2$ ,

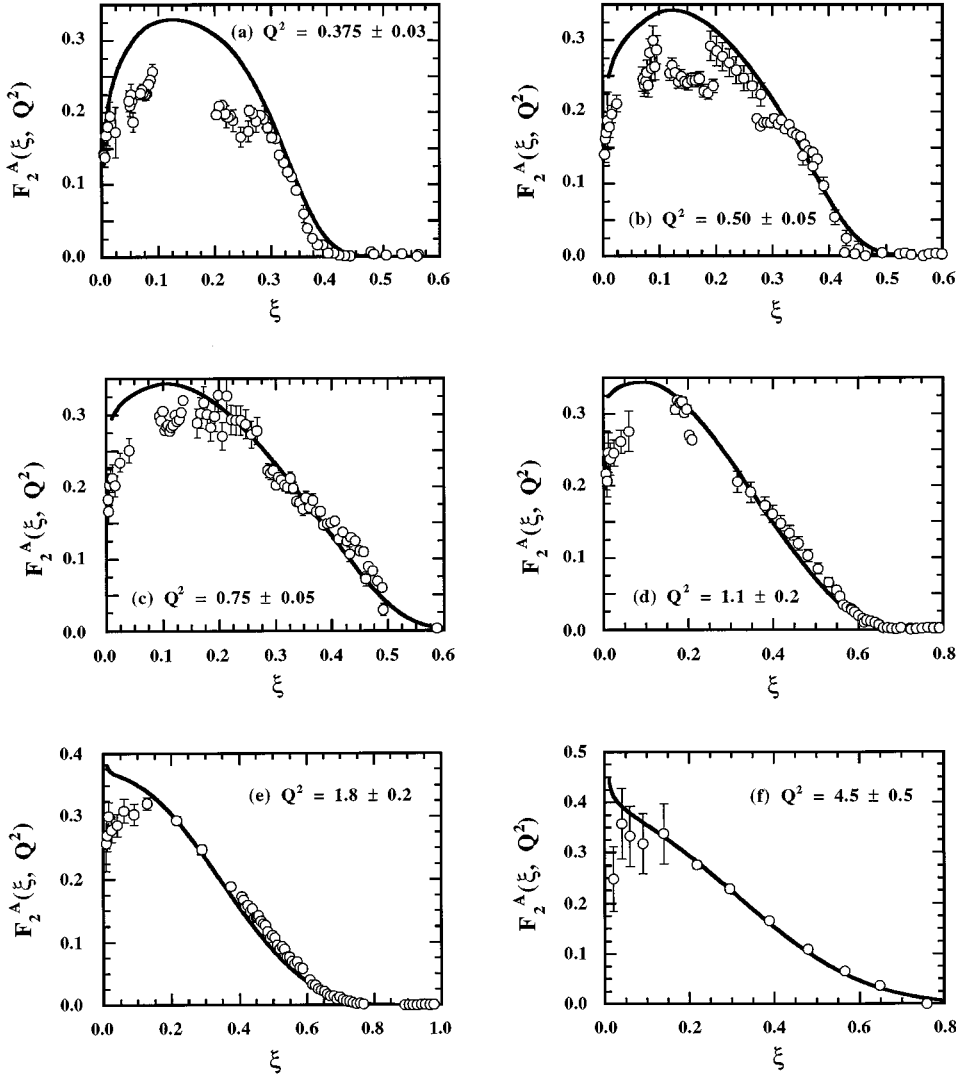


FIG. 4. The same as in Fig. 1, but for the nuclear structure function per nucleon  $F_2^A(\xi, Q^2) \equiv \nu W_2^A(\xi, Q^2)/A$  in the case of nuclei with  $A \approx 12$ . Experimental data are from Refs. [22,23] ( ${}^9\text{Be}$ ), [15,19,24] ( ${}^{12}\text{C}$ ), and [5] ( ${}^{16}\text{O}$ ). The solid curve is the *dual* structure function of the nucleon [Eq. (4)], folded according to the procedure of Ref. [16], which adopts the nucleon spectral function of Ref. [25] to take into account nuclear binding effects.

$1.8 \pm 0.2$ , and  $4.5 \pm 0.5$  ( $\text{GeV}/c$ ) $^2$ . In comparison with the proton and deuteron cases, the most striking feature of our result for nuclei with  $A \approx 12$  is a more rapid smoothing of the resonance bumps with increasing  $Q^2$ , which favors a faster convergence towards the *dual* structure function in the nucleus. This effect, already noticed in Ref. [5] in the  $Q^2$  range 0.1–0.5 ( $\text{GeV}/c$ ) $^2$ , cannot be completely explained as a broadening of the resonance width due to final state interactions, but some extra-damping factor is needed in order to reproduce the missing resonance strength.<sup>1</sup> From Fig. 4 it can clearly be seen that the *dual* structure function (4), properly folded [16] using the nucleon spectral function of Ref. [25], approaches the inelastic data at  $Q^2 \approx Q_0^2 \sim 0.5 - 1.1$  ( $\text{GeV}/c$ ) $^2$ , i.e., for values of  $Q_0^2$  lower than those found in the proton and in the deuteron [ $Q_0^2 \sim 1 - 2$  ( $\text{GeV}/c$ ) $^2$ ].

<sup>1</sup>Medium effects were noticed also in Ref. [26] in the form of a better  $y$  scaling of the inclusive cross section in the region of  $P_{33}(1232)$  resonance electroproduction in nuclei with respect to the free nucleon case.

#### IV. RESULTS AND DISCUSSION

All the data obtained for the structure function  $F_2^p(\xi, Q^2)$  in the proton,  $F_2^D(\xi, Q^2)$  in the deuteron, and  $F_2^A(\xi, Q^2)$  in nuclei with  $A \approx 12$  (see Figs. 1, 2, and 4) show a systematic approach to the properly folded dual structure function for  $\xi \geq 0.2$ , the convergence being even more evident and faster in nuclei, due to the fading of resonances already at  $Q^2 \gtrsim 0.5$  ( $\text{GeV}/c$ ) $^2$ .

At smaller values of  $\xi$  and for  $Q^2 < 5$  ( $\text{GeV}/c$ ) $^2$  proton and deuteron data seem to be compatible with an evolution of sea partons slower than the GRV prediction; in complex nuclei the difference is further enhanced by the shadowing effect [3]. The reason for this discrepancy is not evident and various motivations can be invoked, like a breakdown of duality and/or (unexpected) higher twists at low  $x$  or, more likely, a not yet completely consistent initial [ $Q^2 \approx 0.4$  ( $\text{GeV}/c$ ) $^2$ ] parton density parametrization in a GRV fit [11].

The minimum momentum transfer  $Q_0^2$ , where local duality provides an acceptable fit to the average inclusive inelastic cross sections, should be related to the mass scale  $\mu^2$ , which is defined as the minimum value of  $Q^2$  where the

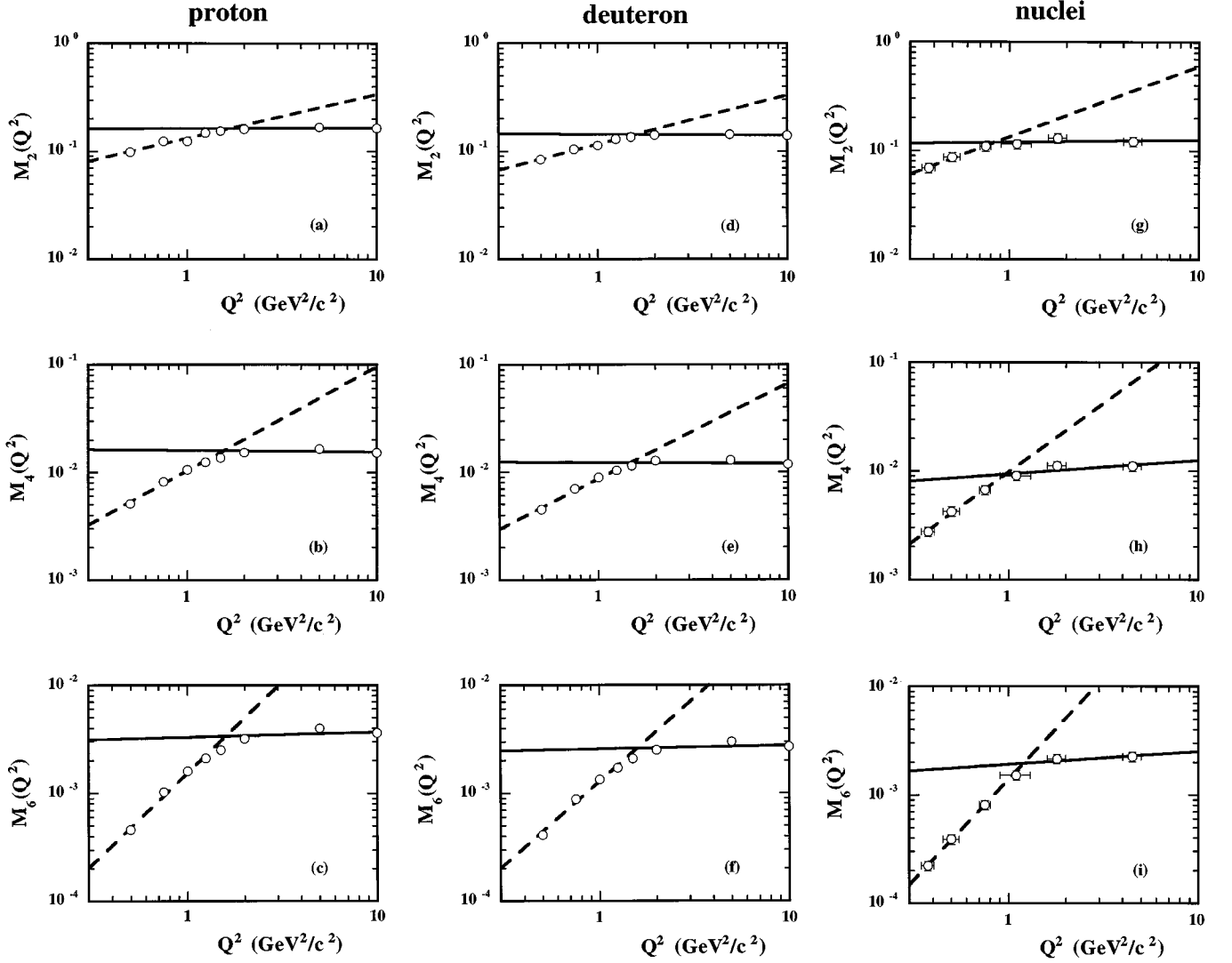


FIG. 5. The moments  $M_2(Q^2)$ ,  $M_4(Q^2)$ , and  $M_6(Q^2)$ , computed according to Eq. (1) for the proton (a),(b),(c), the deuteron (d),(e),(f), and nuclei with  $A \approx 12$  (g),(h),(i) using the experimental data of Figs. 1, 2, and 4, versus  $Q^2$ . The dashed and solid lines are linear fits to low- and high- $Q^2$  points and they are intended to show up the change of the slope of the moments at  $Q^2 \approx Q_0^2$ .

moments of the structure functions  $M_n(Q^2)$  begin to evolve according to twist-2 operators, i.e., when  $M_n(Q^2) \sim A_n(Q^2)$ . Thus, the  $Q^2$  dependence of all the moments should exhibit a systematic change of the slope at  $Q^2 \approx Q_0^2 \approx \mu^2$  and then should follow the perturbative QCD evolution. The *experimental*  $M_2(Q^2)$ ,  $M_4(Q^2)$ , and  $M_6(Q^2)$  moments have been computed for the proton, the deuteron, and nuclei with  $A \approx 12$  according to Eq. (1) using the experimental data for the structure function  $F_2^p(\xi, Q^2)$ ,  $F_2^D(\xi, Q^2)$ , and  $F_2^A(\xi, Q^2)$  shown in Figs. 1, 2, and 4. The results are plotted in Fig. 5 for  $Q^2$  between 0.3 and 5 (GeV/c) $^2$ . The expected systematic change of the slope is clearly exhibited by all the moments considered and the corresponding values of  $Q^2 = Q_0^2$  are reported in Table I. Moreover, in Fig. 6 the relative deviation

$$\frac{\Delta M_n}{A_n}(Q^2) \equiv \frac{M_n(Q^2) - A_n(Q^2)}{A_n(Q^2)} \quad (6)$$

is plotted as a function of  $Q^2$ , where  $A_n(Q^2)$  has been computed from the properly folded *dual* structure function (solid

lines in Figs. 1, 2, and 4). Despite the large errors affecting the available nuclear data, in the case of all the targets considered the results for  $\Delta M_2/A_2$  show a rapid convergence toward  $A_2$  for values of  $Q^2$  very close to the  $Q_0^2$  values of Table I. For higher moments, the convergence toward  $A_n$  is still evident, but it is slower probably because of the presence of resonances at large  $\xi$ .

The results presented in Figs. 5 and 6 correspond only to the contribution of the inelastic part of the structure functions

TABLE I. Values of  $Q^2 = Q_0^2$  (in GeV $^2/c^2$ ) where a systematic change in the slope is exhibited by the  $Q^2$  dependence of the moments  $M_2(Q^2)$ ,  $M_4(Q^2)$ , and  $M_6(Q^2)$  (see Fig. 5), computed for the proton, the deuteron, and nuclei with  $A \approx 12$  according to Eq. (1) using the experimental data shown in Figs. 1, 2, and 4.

	$M_2$	$M_4$	$M_6$
Proton	$1.6 \pm 0.2$	$1.5 \pm 0.1$	$1.6 \pm 0.1$
Deuteron	$1.6 \pm 0.1$	$1.5 \pm 0.1$	$1.5 \pm 0.1$
Nuclei	$0.8 \pm 0.1$	$1.0 \pm 0.2$	$1.2 \pm 0.1$

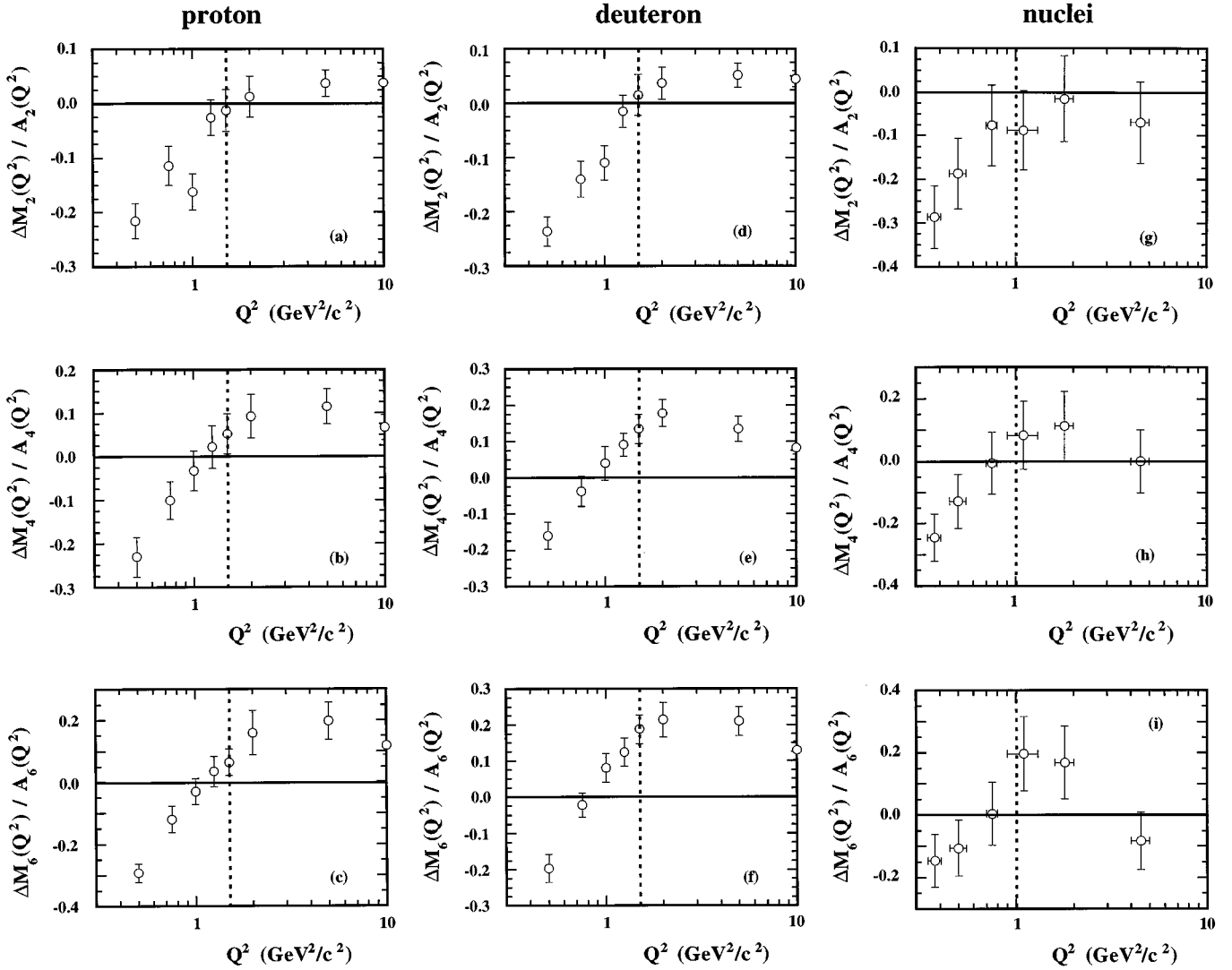


FIG. 6. The relative deviation  $\Delta M_n(Q^2)/A_n(Q^2)$  [Eq. (6)] of the *experimental* moments  $M_n(Q^2)$ , reported in Fig. 5, with respect to the leading twist moments  $A_n(Q^2)$ , calculated from Eq. (1) using the *dual* nucleon structure function (4), properly folded [16], with the nucleon motion in the nuclear medium. The vertical dotted lines are intended to show the approximate location of the static point  $Q^2 \approx \mu^2$ , namely,  $\mu_N^2 \approx \mu_D^2 \approx 1.5$  (GeV/c)<sup>2</sup> and  $\mu_A^2 \approx 1.0$  (GeV/c)<sup>2</sup> (see the text).

to the moments (1). Since in Eq. (1) the integration is extended up to  $\xi=1$ , the question of the role played by the contribution of the elastic peak in the nucleon and the quasielastic peak in nuclei naturally arises. Therefore, in the case of the proton we have considered the contribution  $M_n^{(\text{el})}(Q^2)$  resulting from the elastic peak, which reads as

$$M_n^{(\text{el})}(Q^2) = \frac{G_E^2(Q^2) + \tau G_M^2(Q^2)}{1 + \tau} \frac{\xi_p^n}{2 - \xi_p}, \quad (7)$$

where  $G_E$  ( $G_M$ ) is the charge (magnetic) Sachs form factor of the proton,  $\xi_p \equiv \xi(x=1) = 2/(1 + \sqrt{1 + 1/\tau})$ , and  $\tau = Q^2/4m^2$ . In Fig. 7 we have reported the results obtained for  $M_n^{(\text{tot})}(Q^2) \equiv M_n^{(\text{el})}(Q^2) + M_n(Q^2)$  and  $\Delta M_n^{(\text{tot})}(Q^2)/A_n(Q^2)$ .<sup>2</sup> It can clearly be seen that the higher twists introduced by the proton elastic peak do not change significantly (within few percent) the lowest-order moment  $M_2(Q^2)$  for

$Q^2 \gtrsim 1.5$  (GeV/c)<sup>2</sup>, whereas they sharply affect higher moments up to quite large values of  $Q^2$  (cf. also Ref. [8]). This means that parton-hadron duality still holds for the total area  $M_2^{(\text{tot})}(Q^2)$ , i.e., for the average of the structure function over all possible final states, with a mass scale consistent with the one obtained including the inelastic channels only. On the contrary, at least for  $Q^2$  up to several (GeV/c)<sup>2</sup> the local duality is violated by the elastic peak. This result is consistent with those of Refs. [1,6], where the applicability of the concept of parton-hadron local duality in the region around the nucleon elastic peak was found to be critical. We have obtained similar results in the case of the deuteron, while the

<sup>2</sup>We point out that Eq. (3) holds only for  $M_n^{(\text{tot})}(Q^2)$  (cf. Ref. [8]). The elastic contribution (7) *must* be included in Eq. (1) when the extraction of the higher twists from the moments is required, which is not the case of the present work.

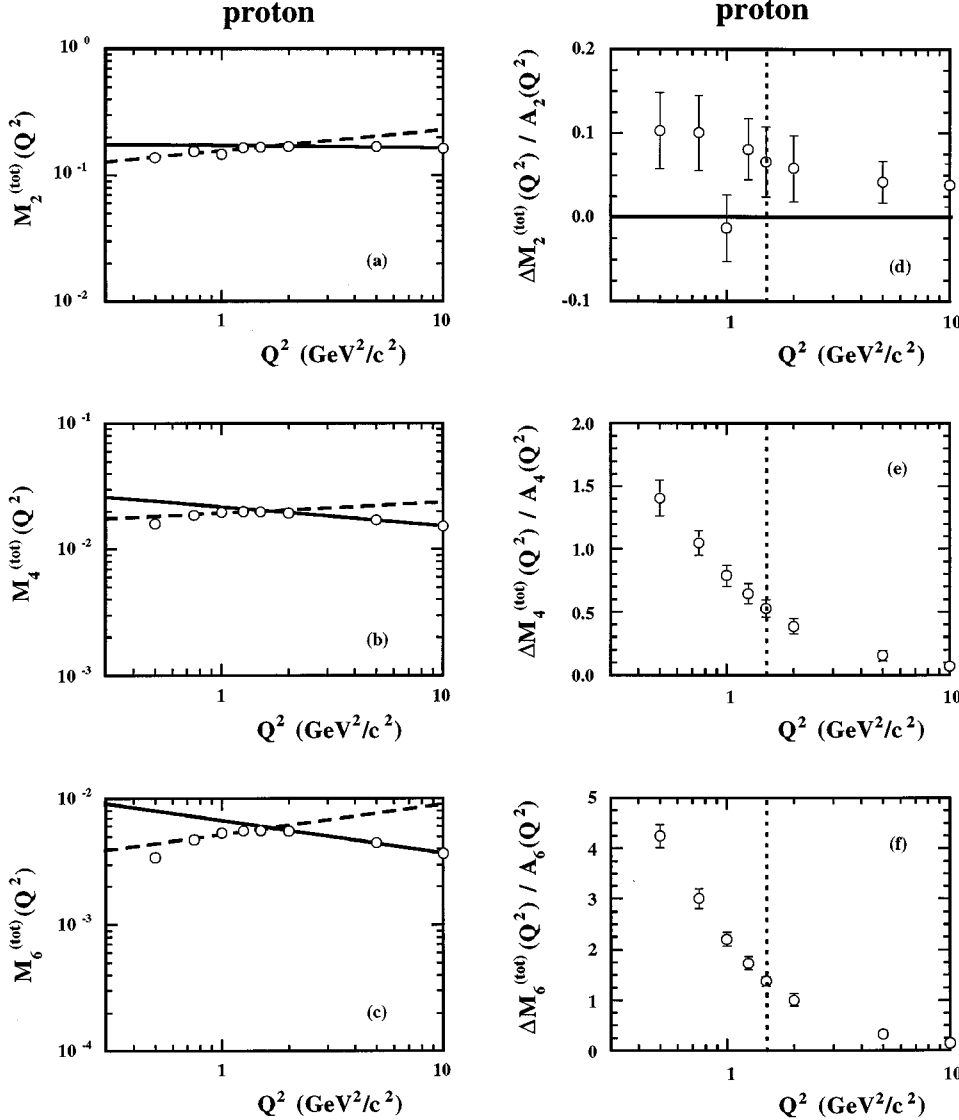


FIG. 7. The moments  $M_n^{(\text{tot})}(Q^2) = M_n^{(\text{el})}(Q^2) + M_n(Q^2)$  (a),(b),(c) and the relative deviation  $\Delta M_n^{(\text{tot})}(Q^2)/A_n(Q^2)$  (d),(e),(f), calculated for the proton including in Eq. (1) the contribution of the elastic peak (7), versus  $Q^2$ . The vertical dotted lines are the same as in Figs. 6(a)–6(c).

analysis of the available nuclear data appears to be compatible within large errors. To sum up, the twist-2 moments  $A_n(Q^2)$  dominate the total moments  $M_n^{(\text{tot})}(Q^2)$  starting from values of  $Q^2$  which strongly depend upon the order of the moment (see Fig. 7). On the contrary, the  $Q^2$  behavior of the inelastic contribution  $M_n(Q^2)$  is governed by  $A_n(Q^2)$  starting from a value  $Q^2 \approx Q_0^2$  almost independent of the order of the moment (see Figs. 5 and 6); thus, after Mellin transformation, the twist-2 operators dominate the inelastic part of the structure function for  $Q^2 \geq Q_0^2$  and, therefore, the parton-hadron local duality holds for the averages of the structure function over the nucleon-resonance bumps.

Both the comparison of the moments and the discussion on the onset of the local duality strongly suggest the occurrence of the dominance of twist-2 operators in the inelastic structure functions for values of  $Q^2$  above the  $Q_0^2$  values of Table I. Therefore, we may argue that present experimental data are compatible with a mass scale  $\mu^2 \approx Q_0^2$ ; from Table I this means  $\mu_N^2 \approx \mu_D^2 = 1.5 \pm 0.1$  (GeV/c)<sup>2</sup> for the nucleon and the deuteron, and  $\mu_A^2 = 1.0 \pm 0.2$  (GeV/c)<sup>2</sup> for nuclei with  $A \approx 12$ .

A change of the mass scale of the twist-2 matrix elements in nuclei ( $\mu_A^2 < \mu_D^2 \approx \mu_N^2$ ) is expected to lead to a rescaling relation for the (inelastic) moments [27,28], viz.,

$$M_n^A(Q^2) = M_n^D(\delta_n(Q^2) \cdot Q^2), \quad (8)$$

with  $\delta_n(Q^2 \approx \mu^2) \approx \mu_D^2/\mu_A^2$ . Assuming a rescaling factor  $\delta_n(\mu^2) \approx \delta$  independent of the order of the moment, the rescaling relation (8) with  $\delta = 1.17 \pm 0.09$  brings all the moments in the deuteron and in nuclei into the best simultaneous agreement around the mass scale region, as is shown in Fig. 8. A possible mechanism for the  $Q^2$  rescaling has been suggested in Ref. [27]: The quark confinement scale may increase in going from a free nucleon to a nucleus, due to the partial overlap of nucleons in the nuclear medium. The change in the quark confinement size leads to a change in the mass scale  $\mu^2$  and one gets  $\delta = \mu_D^2/\mu_A^2 = \lambda_A^2/\lambda_D^2$ , where  $\lambda_D$  ( $\approx \lambda_N$ ) and  $\lambda_A$  are the average quark confinement size in the deuteron (nucleon) and in the nucleus, respectively. We stress that the partial quark deconfinement is not the only mechanism yielding a rescaling effect; in this respect, we



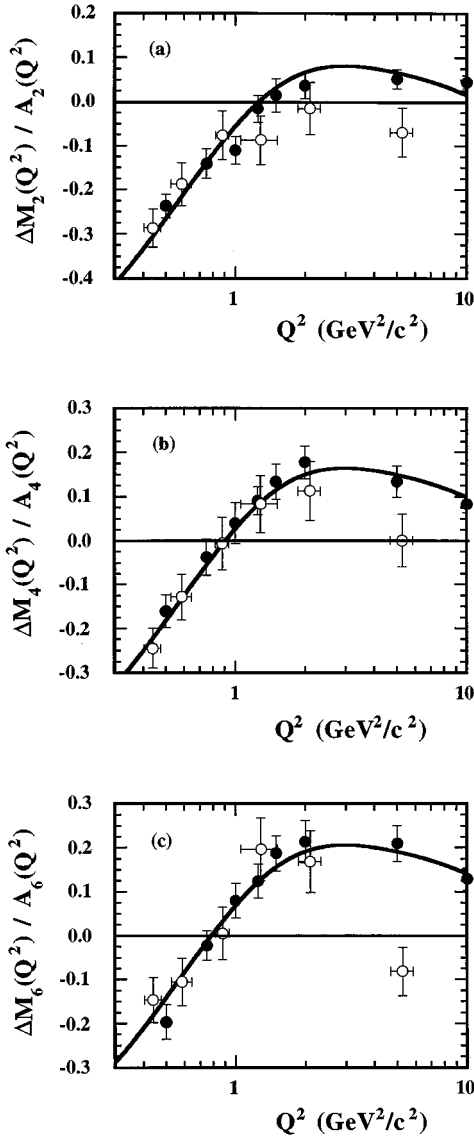


FIG. 8. The relative deviation  $\Delta M_n(Q^2)/A_n(Q^2)$  [Eq. (6)] of the *experimental* moments  $M_n(Q^2)$  calculated for the deuteron (solid circles) and for nuclei with  $A \approx 12$  (open circles). The latter have been  $Q^2$  rescaled according to Eq. (8) using  $\delta_n(Q^2 \approx \mu^2) \approx \mu_D^2/\mu_A^2 = 1.17$ . The solid lines represent global fits of the deuteron and ( $Q^2$  rescaled) nuclear points.

mention also the model of Ref. [28], where the rescaling mechanism is driven by the off mass shellness of the nucleon in the nucleus.

If  $\delta_n(Q^2)$  is independent of the order of the moment, then after Mellin transformation the  $Q^2$  rescaling can be applied to the nuclear structure function per nucleon  $F_2^A(x, Q^2)$ , viz.,

$$F_2^A(x, Q^2) = F_2^D(x, \delta(Q^2) \cdot Q^2), \quad (9)$$

where the virtual photon mass dependence of  $\delta(Q^2)$  follows from perturbative QCD evolution at NLO (see [27,28]). In Fig. 9 existing data on  $F_2^A(x, Q^2)$  for nuclei with  $A \approx 12$  are plotted for fixed values of  $x$  in a wide  $Q^2$  range. The *dual* structure function (4), properly folded [16] for taking into account nuclear binding effects, is also shown in Fig. 9 for different values of the mass scale ratio  $\mu_D/\mu_A$ . It can be

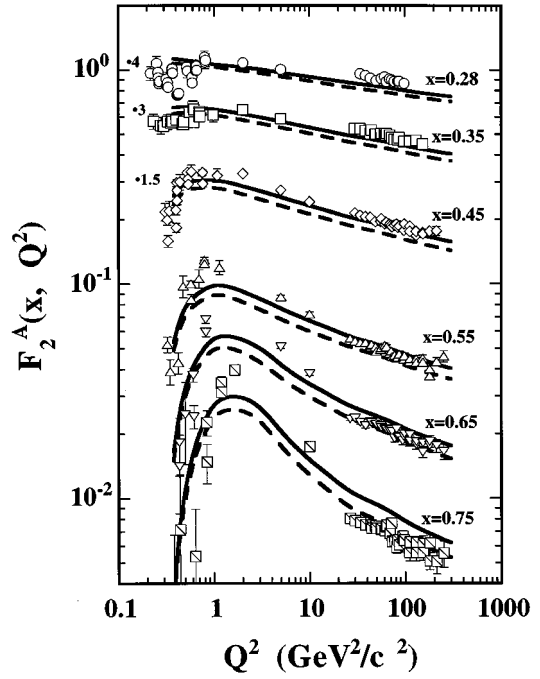


FIG. 9. Nuclear structure function per nucleon  $F_2^A(x, Q^2) \equiv \nu W_2^A(x, Q^2)/A$  versus  $Q^2$  at fixed values of  $x$  in case of nuclei with  $A \approx 12$ . The experimental data are from Refs. [5,15,19,22–24,30]. The various markers correspond to different values of  $x$ . The solid line is the folding of the *dual* nucleon structure function [Eq. (4)] obtained using the procedure of Ref. [16]. The dashed line is the same as the solid line, but using the rescaling relation (9) with  $\delta(Q^2)$  taken from Ref. [27] and  $\mu_D/\mu_A = 1.10$ .

seen that at high  $Q^2$  a mass scale ratio  $\mu_D/\mu_A = 1.1$  removes most of the disagreement at large  $x$ , but at the price of spoiling the agreement at intermediate values of  $x$ . Moreover, at low values of  $Q^2$  the present accuracy of the data does not allow any serious discrimination between different quark confinement ratios. We mention that in Ref. [29] a nucleon swelling corresponding to  $\mu_D/\mu_A \approx 1.075$  has been derived from a combined analysis of the EMC effect at small and large  $x$ , performed within a constituent-quark picture of the nucleon structure function in nuclei.

To sum up, roughly consistent values of the mass scale ratio  $\mu_D/\mu_A$  between the deuteron and nuclei with  $A \approx 12$  can be obtained in different ways, viz., (i) from the onset of local duality (see Table I and Fig. 5):  $\mu_D/\mu_A = 1.2 \pm 0.1$ ; (ii) from the rescaling of the moments at the static point  $Q^2 \approx \mu^2$  (see Fig. 8),  $\mu_D/\mu_A = 1.08 \pm 0.05$ ; (iii) from the EMC effect (see Fig. 9),  $\mu_D/\mu_A \approx 1.10$ .

Nucleon resonances contribute mostly to  $M_4(Q^2)$  and  $M_6(Q^2)$  (see Fig. 6): The good overlap of these moments in the deuteron and nuclei, observed in Fig. 8 after  $Q^2$  rescaling, could suggest that a change of the mass scale in nuclei might be consistent with the more rapid decrease of the inelastic  $P_{33}(1232)$  and  $D_{13}(1520)$  resonance form factors claimed in Ref. [5], where values of  $Q^2$  as low as  $0.1 (\text{GeV}/c)^2$  are, however, involved. The *experimental* suppression factor  $R_s(Q^2)$ , as determined in Ref. [5] using inclusive  $^{12}\text{C}$  and  $^{16}\text{O}$  data, is reported in Fig. 10 as a function of  $Q^2$  in the region of the  $P_{33}(1232)$  resonance production. Assuming that a constant  $Q^2$  rescaling  $\delta(Q^2)$

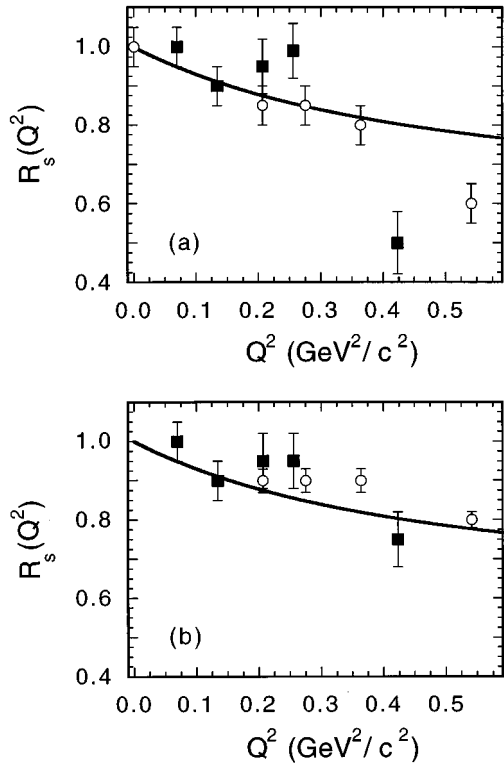


FIG. 10. The suppression factor  $R_s(Q^2)$  versus  $Q^2$ , as determined in Ref. [5], using inclusive  $^{12}\text{C}$  (open circles) and  $^{16}\text{O}$  data (solid squares), in the case of the excitation of the  $P_{33}(1232)$  resonance only (a) and for the total inclusive cross section at  $W = 1232$  MeV (b). The solid line is the prediction of the rescaling relation (10), obtained adopting a dipole ansatz for the magnetic form factor of the  $N$ - $\Delta$  transition,  $G_M^{(N-\Delta)}(Q^2)$ , and the value  $\mu_D/\mu_A = 1.08$ .

$\approx \mu_D^2/\mu_A^2$  can be used below the static point ( $Q^2 < \mu^2$ ), the suppression factor is expected to be given by

$$R_s(Q^2) = \left\{ \frac{G_M^{(N-\Delta)}[(\mu_D^2/\mu_A^2) Q^2]}{G_M^{(N-\Delta)}(Q^2)} \right\}^2, \quad (10)$$

where  $G_M^{(N-\Delta)}(Q^2)$  is the magnetic form factor of the  $N$ - $\Delta$  transition. Using a standard dipole form (for the sake of simplicity) and the value  $\mu_D/\mu_A = 1.08$ , one gets the solid lines shown in Fig. 10 at  $Q^2 \lesssim 0.5$  ( $\text{GeV}/c$ ) $^2$ . It can be seen that (surprisingly) a simple  $Q^2$  rescaling of the dipole ansatz is consistent with the quenching observed for the  $\Delta$ -resonance electroproduction both in case of the excitation strength alone [see Fig. 10(a)] and for the total inclusive cross section [see Fig. 10(b) and cf. Ref. [31]].

A  $Q^2$ -rescaling effect could in principle be applied also to the elastic form factors of a nucleon bound in a nucleus and it can be viewed as a change of the nucleon radius in the nuclear medium. In this respect, it should be pointed out that (i) in Ref. [32] an increase not larger than  $\approx 6\%$  of the proton charge radius was found to be compatible with  $y$  scaling in  $^3\text{He}$  and  $^{56}\text{Fe}$ , (ii) the analysis of the Coulomb sum rule (CSR) made in Ref. [33] suggested an upper limit of  $\approx 10\%$  to the variation of the proton charge radius in  $^{56}\text{Fe}$ , and (iii) recently [34] the experimental value ( $S_L$ ) of the CSR in  $^{12}\text{C}$

and  $^{56}\text{Fe}$  has been accurately analyzed at  $Q^2 \approx 0.3$  ( $\text{GeV}/c$ ) $^2$ , obtaining a saturation value  $S_L = 0.94 \pm 0.13$  and  $S_L = 0.97 \pm 0.12$ , respectively. If at the same value of  $Q^2$  we would assume the same change of the mass scale ( $\mu_D^2/\mu_A^2 \approx 1.15$ ) observed in the inelastic channels, an increase of  $\approx 8\%$  for the proton charge radius and a quenching of  $\approx 0.84$  for  $S_L$  would be obtained, both being at the limit with the quoted errors. However, based on the results shown in Figs. 5–7, it is unlikely that a common  $Q^2$ -rescaling effect could be applied both to the nucleon elastic peak and to the nucleon-resonance transitions.

Before closing, let us make a brief comment on the photoproduction of nucleon resonances. Real photon experiments [35] show that in several nuclei [36] a substantial reduction of the excitation strength of  $D_{13}(1520)$  and  $F_{15}(1680)$  resonances occur in comparison with the corresponding hydrogen and deuterium data. This effect suggests both a broadening of the resonance width and a quenching of their excitation strength [37]; while the broadening could be a consequence of final state interactions [38], the quenching might be ascribed to a reduction of the transition strength in radial-type excitations, due again to the overlap of confinement potentials among neighboring nucleons in nuclei [39]. However, a common explanation of the behavior of the resonance bumps both in the photoproduction and in the electroproduction still awaits for a deeper understanding.

## V. CONCLUSIONS

The concept of parton-hadron local duality represents a very powerful tool for analyzing inclusive lepton scattering data in the low- $Q^2$  region, where important quantities like the mass scale, the leading twist, and higher twist in the structure function may be investigated. We have analyzed all the existing inclusive data on the inelastic structure function of the nucleon, the deuteron, and light complex nuclei in a  $Q^2$  range 0.3–5 ( $\text{GeV}/c$ ) $^2$  and the  $Q^2$  behaviors of the structure function and its moments have been presented for all the targets considered. In the case of the proton we have observed that the Bloom-Gilman local duality is fulfilled only by the inelastic part of the structure function, while the inclusion of the contribution of the elastic peak leads to remarkable violations of the local duality. In the case of complex nuclei, despite the poor statistics of the available data, our analysis suggests that the onset of the parton-hadron local duality for the inelastic part of the structure function is anticipated with respect to the case of the nucleon and the deuteron. A possible interpretation of this result in terms of a  $Q^2$ -rescaling effect has been discussed: Using different methods, a decrease of the mass scale of  $\approx 8\%$  in nuclei turns out to be consistent with inelastic experimental data. It has also been shown that the same variation of the mass scale is consistent with the faster falloff of the  $P_{33}(1232)$  transition form factors observed in nuclei with respect to the nucleon case even at very low values of  $Q^2$ . Finally, we expect that the same  $Q^2$ -rescaling effect cannot be applied both to the elastic and transition form factors of a nucleon bound in a nucleus, consistently with the severe constraints on nucleon swelling arising from updated analyses of the Coulomb sum rule in nuclei.

In conclusion, the Bloom-Gilman local duality in nucleon

and nuclei appears to be a nontrivial dynamical property of the inelastic structure functions, whose deep understanding is still to be reached and deserves much more attention from the theoretical as well as the experimental point of view. As to the latter, more systematic and high-precision inclusive data are needed for a clear-cut extraction of information; our present analysis should therefore be considered as a strong

suggestion that interesting results can be expected, when the structure functions of nucleon and nuclei are compared in the low- $Q^2$  region. New facilities becoming operative in the next future, like CEBAF, are expected to provide inclusive data with unprecedented accuracy, allowing a throughout investigation of the relation among the physics in the nucleon-resonance and deep inelastic scattering regions.

- 
- [1] E. Bloom and F. Gilman, Phys. Rev. Lett. **25**, 1140 (1970); Phys. Rev. D **4**, 2901 (1971).
- [2] J.M. Laget, in *New Vistas in Electro-Nuclear Physics*, edited by E.L. Tomusiak, H.S. Coplan and E.T. Dressler, Vol. 142 of *NATO Advanced Study Institute, Series B: Physics* (Plenum, New York, 1986), pp. 361–429, and references therein.
- [3] M. Arneodo, Phys. Rep. **260**, 302 (1994), and references therein.
- [4] F. Heimlich *et al.*, Nucl. Phys. **A231**, 509 (1974).
- [5] M. Anghinolfi *et al.*, Nucl. Phys. **A602**, 405 (1996); J. Phys. G **21**, L9 (1995).
- [6] A. De Rujula, H. Georgi, and H.D. Politzer, Ann. Phys. (N.Y.) **103**, 315 (1977).
- [7] H. Georgi and H.D. Politzer, Phys. Rev. D **14**, 1829 (1976).
- [8] X. Ji and P. Unrau, Phys. Rev. D **52**, 72 (1995).
- [9] M. Arneodo *et al.*, Phys. Lett. B **364**, 107 (1995); L.W. Whitlow *et al.*, *ibid.* **282**, 475 (1992); M. Virchaux and A. Milsztajn, *ibid.* **274**, 221 (1992).
- [10] G. Altarelli and G. Parisi, Nucl. Phys. **B126**, 298 (1977).
- [11] M. Gluck, E. Reya, and A. Vogt, Z. Phys. C **53**, 127 (1992); **67**, 433 (1995); H. Plochow-Besch, Report No. CERN-PPE/15-3-1995 (PDF Library); Comput. Phys. Commun. **75**, 396 (1993).
- [12] G. Altarelli, R.K. Ellis, and G. Martinelli, Nucl. Phys. **B143**, 521 (1978); **B157**, 461 (1979).
- [13] J.L. Miramontes, M.A. Miramontes, and J. Sanchez Guillen, Phys. Rev. D **40**, 2184 (1989); Z. Phys. C **41**, 247 (1988).
- [14] K. Bitar, P.W. Johnson, and Wu-Ki Tung, Phys. Lett. **83B**, 114 (1979); R.K. Ellis, L. Petronzio, and G. Parisi, *ibid.* **64B**, 97 (1976).
- [15] A. Bodek *et al.*, Phys. Rev. D **20**, 7 (1979); S. Stein *et al.*, Phys. Rev. D **12**, 1884 (1975).
- [16] S. Simula, Few-Body Syst., Suppl. **8**, 423 (1995); **9**, 466 (1995).
- [17] L.L. Frankfurt and M.I. Strikman, Phys. Rep. **76**, 215 (1981).
- [18] M. Lacombe *et al.*, Phys. Lett. **101B**, 139 (1981).
- [19] M. Arneodo *et al.*, Nucl. Phys. **B333**, 1 (1990).
- [20] D.T. Baran *et al.*, Phys. Rev. Lett. **61**, 400 (1988).
- [21] E. Rondio (private communication).
- [22] J. Gomez *et al.*, Phys. Rev. D **49**, 4348 (1994).
- [23] J. Franz *et al.*, Z. Phys. C **10**, 105 (1981).
- [24] (a) D.B. Day *et al.*, Phys. Rev. C **48**, 1849 (1993); (b) F. Heimlich *et al.*, *ibid.* **3**, 1448 (1971); (c) R.M. Sealock *et al.*, Phys. Rev. Lett. **62**, 1350 (1989).
- [25] C. Ciofi and S. Simula, Phys. Rev. C **53**, 1689 (1996); Phys. Lett. B **325**, 276 (1994).
- [26] R. Cenni and P. Saracco, J. Phys. G **20**, 727 (1994).
- [27] R. Jaffe Phys. Rev. Lett. **50**, 228 (1983); F.E. Close, R.G. Roberts, and G.G. Ross, Phys. Lett. **129B**, 346 (1983); F. Close, R. Jaffe, A. Roberts, and G. Ross, Phys. Lett. **134B**, 449 (1984); Phys. Rev. D **31**, 1004 (1985).
- [28] G.V. Dunne and A. W. Thomas, Nucl. Phys. **A455**, 701 (1986).
- [29] W. Zhu and L. Qian, Phys. Rev. C **45**, 1397 (1992).
- [30] A.C. Benvenuti *et al.*, Phys. Lett. B **195**, 91 (1987).
- [31] C.E. Carlson and N.C. Mukhopadhyay, Phys. Rev. D **47**, R1737 (1993).
- [32] I. Sick, Phys. Lett. **157B**, 13 (1985).
- [33] J.P. Chen *et al.*, Phys. Rev. Lett. **66**, 1283 (1991).
- [34] J. Jourdan, Nucl. Phys. **A603**, 117 (1996).
- [35] M. Anghinolfi *et al.*, Phys. Rev. C **47**, R922 (1993); Th. Frommhold *et al.*, Phys. Lett. B **295**, 28 (1992); G. Ricco, in *Proceedings of the 4th International Seminar on Nuclear Physics*, Amalfi, Italy, 1992, edited by A. Covello (World Scientific, Singapore, 1993), p. 57.
- [36] M. Bianchi *et al.*, Phys. Lett. B **299**, 219 (1993); **325**, 333 (1994).
- [37] V. Mokeev, E. Santopinto, M. Giannini, and G. Ricco, Int. J. Mod. Phys. E **4**, 607 (1995).
- [38] W.M. Alberico, G. Gervino, and A. Lavagno, Phys. Lett. B **231**, 177 (1994); L. Kondratyuk, M. Krivoruchenko, N. Bianchi, E. De Sanctis, and V. Muccifora, Nucl. Phys. **A579**, 453 (1994).
- [39] M. Giannini and E. Santopinto, Phys. Rev. C **49**, R1258 (1994); M. Giannini and E. Trovatore, Int. J. Mod. Phys. E (to be published).